Journal of Optoelectronics and Advanced Materials Vol. 7, No. 5, October 2005, p. 2427 - 2434

SURFACE WAVE SUSTAINED DISCHARGE IN ARGON: TWO-TEMPERATURE COLLISIONAL-RADIATIVE MODEL AND EXPERIMENTAL VERIFICATION

H. Nowakowska*, D. Czylkowski, Z. Zakrzewski

The Szewalski Institute of Fluid-Flow Machinery, Polish Academy of Sciences, Fiszera 14, 80-231 Gdansk, Poland

Two-temperature collisional-radiative model of surface-wave sustained discharge at atmospheric pressure in a capillary tube is presented. Division of microwave power within the discharge is analysed. Calculations are made for atmospheric pressure argon plasma created inside a quartz tube with and without a liquid cooling coat and a shielding grid. Wave attenuation characteristics and axial distributions of density of dissipated power are presented. The predicted dependence of discharge length on the total flux of wave power is compared with the experimental values.

(Received January 21, 2005; accepted September 22, 2005)

Keywords: Microwave discharge, Low temperature plasma, Surface wave, Modelling

1. Introduction

In the last decades discharges sustained by the electromagnetic field of a wave propagating along the plasma, especially those sustained by surface waves (SW), have been intensively investigated. The modelling of low-pressure surface wave discharges (SWD) is far advanced and the state of the art is well documented [1-9]. The modelling of discharges sustained by surface waves at atmospheric pressure for many years (for example [10,11]) has not been keeping pace with experimental investigations and applications, which have been reported. The situation changed recently, when some interesting articles concerning different aspect of such a modelling were published. A self-consistent model of non-equilibrium spherical microwave discharges has been presented in [12,13]. Papers [14-17] deal with non-equilibrium models of long discharge and with propagation of electromagnetic wave along a plasma filament. In [18,19], a numerical fluid-plasma model of SWD and an attempt of explanation contraction phenomenon are presented.

The present paper concerns a cylindrical SWD in argon with special attention to the division of microwave power in the discharge region and to determine the plasma column length versus absorbed microwave power.

A self-consistent model would require simultaneous solving of the Maxwell equations and of the equations describing the discharge processes. A commonly used simplifying approximation is to assume that the influence of any axial gradient on both the discharge maintenance processes and wave propagation is negligible. This is as an *approximation of local axial uniformity* [4] and it is applicable if the condition $2\alpha(L)a << 1$ is fulfilled, where α is the wave attenuation coefficient, a – the inner radius of discharge tube and L – the power lost per unit length of the plasma column.

The assumption of local axial uniformity allows to perform the calculations in two separate stages and then to merge the results. The first stage deals with energy transfer from the wave, via plasma, to the environment. For any axial position the solution of the problem is the same as that for an axially uniform discharge. As a result one obtains the radial distributions of all the plasma parameters for given discharge conditions (the gas composition and pressure, the wave mode and

* Corresponding author: helena@imp.gda.pl

frequency, the tube transverse dimensions and the wall material) for consecutive values of L. Therefore, these calculations provide also functional dependence of $\alpha(L)$, which is determined using the standard methods of electromagnetic field theory.

The second stage of the calculations concerns the gradual transfer of power from the wave field to the plasma as the wave propagates along the column. It links the local maintenance processes occurring in elementary slabs of the discharge with the overall power balance in the plasma column and provides the axial distribution of the power loss L for given total power P_0 delivered by the wave to the plasma.

Let us define cylindrical coordinates (z, r, ϕ) such that z coincides with the plasma column axis and r is the distance from that axis. The angular coordinate ϕ is irrelevant because of the axial symmetry of the system. Then the axial distribution of the power loss is $L(z)$ and can be found [4] from

$$\frac{\mathrm{d}L(z)}{\mathrm{d}z} = -2\alpha(L)L(z)\left[1 - \frac{L(z)}{\alpha(L)}\frac{\mathrm{d}\alpha(L)}{\mathrm{d}L}\right]^{-1}, \tag{1}$$

with the initial condition $L_0 \equiv L(0) = 2\alpha(L_0)P_0$, where $P_0 = P(0)$ and P is the power flux of the SW and z=0 corresponds to the beginning of the column. This result, merged with the radial distribution of plasma parameters for a given value of L obtained from the analysis of an axially uniform discharge, provides complete information about the spatial distribution of plasma parameters.

2. Model of an axially uniform discharge in argon at atmospheric pressure

For the description of microwave discharge maintenance processes we adopt a two-temperature model of Lelevkin *et al.* [20, chap 7.8]. Unlike in the model developed in [11], we do not use the Saha equation. Instead, we employ the continuity equation together with coefficients from collisional-radiative model [21]. Additionally, we take into account the ambipolar diffusion.

If the radiative energy loss and the gas flow are neglected, the energy conservation equations, for the heavy particles and the electrons have the form:

$$\frac{3}{2}\delta\nu nk(T_e - T_h) = -\frac{1}{r}\frac{\mathrm{d}}{\mathrm{d}r}\left(r\lambda\frac{\mathrm{d}T_h}{\mathrm{d}r}\right), \tag{2}$$

$$\sigma E^2 = \frac{3}{2}\delta\nu nk(T_e - T_h) - \frac{1}{r}\frac{\mathrm{d}}{\mathrm{d}r}\left(r\lambda_e\frac{\mathrm{d}T_e}{\mathrm{d}r} - r\upsilon n\left(\frac{5}{2}kT_e + U_I\right)\right). \tag{3}$$

Here T_h and T_e are heavy particles and electrons temperatures, respectively, δ is the fraction of electron energy lost in collision of an electron with a heavy particle, ν is the effective frequency of elastic collisions of electrons, n is the electron number density and k is the Boltzmann constant. The coefficients λ and λ_e designate the thermal conductivities for the heavy particles and electrons, respectively, σ is the electrical conductivity, E is the electrical field intensity (rms value), U_I is the energy of ionisation, $\upsilon = -(D/n)(\mathrm{d}n/\mathrm{d}r)$ is the ambipolar diffusion velocity with D being the ambipolar diffusion coefficient. The above plasma parameters for a two-temperature argon plasma were calculated like in [20], taking into account data from [22,23].

The continuity equation for electrons can be written as

$$\frac{1}{r}\frac{\mathrm{d}}{\mathrm{d}r}\left(rD\frac{\mathrm{d}n}{\mathrm{d}r}\right) + S_{CR}\cdot n\cdot n_a - \alpha_{CR}n\cdot n_i = 0, \tag{4}$$

where S_{CR} and α_{CR} are the ionisation and recombination coefficients. They are determined using formulas and data from [21] where they were determined from collisional-radiative (CR) model of Benoy *et al.* [24] for argon. In this model the number of excited states in argon is reduced to 21.

The number densities of atoms and ions, n_a and n_i, respectively, are determined using on the Dalton law $p/kT_\mathrm{h} = n_a + n_\mathrm{i} + nT_e/T_h$, where p denotes the pressure, and condition of quasi-neutrality of the plasma $n \approx n_i$. For discharges in capillary tubes the skin effect may be in most cases neglected and the electric field intensity E may be regarded as constant in the radial direction. In this approximation the power deposited in the plasma, per unit length of the column, is:

$$L = 2\pi \int_0^a \sigma E^2 r dr \cong 2\pi E^2 \int_0^a \sigma r dr \,. \tag{5}$$

Validity of the assumptions of a negligible influence of the skin effect and radiation has been checked *ex post* after having made calculations for specific discharge conditions.

The following boundary conditions are adopted: At the tube axis (r=0) there is, owing to the axial symmetry,

$$\frac{\mathrm{d}T_e}{\mathrm{d}r} = 0, \qquad \frac{\mathrm{d}T_h}{\mathrm{d}r} = 0 \quad \text{and} \quad \frac{\mathrm{d}n}{\mathrm{d}r} = 0 \,. \tag{6}$$

At the inner surface of the wall (r=a) the heavy particles lose their energy to the wall, therefore

$$\lambda \frac{\mathrm{d}T_h}{\mathrm{d}r} = \lambda_w \frac{\mathrm{d}T_w}{\mathrm{d}r} \,, \tag{7}$$

where λ_w and T_w are the thermal conductivity of the wall material and the temperature of the wall inner surface, respectively. The latter is related to the temperature T_∞ of the outer surface of the tube wall by

$$T_w = T_\infty + L \cdot \frac{\ln(b/a)}{2\pi\lambda_w} \,, \tag{8}$$

where b is the outer diameter of the discharge tube. For the electron gas the wall surface at r=a may be treated as an adiabatic envelope, as it can be assumed that electrons are reflected by the electric field within the sheath and do not reach the wall. Therefore no energy is transferred from the electron gas to the wall and, for r=a, we can set

$$\lambda_e \frac{\mathrm{d}T_e}{\mathrm{d}r} = 0 \quad \text{and} \quad \frac{\mathrm{d}n}{\mathrm{d}r} = 0 \,. \tag{9}$$

Equations (2) – (4) are converted into a set of differential equations of the first order and solved, for a range of values of L and given ω, a, b, λ_w, p and T_∞. This yields, for each L, radial distributions $T(r)$, $T_e(r)$ and $n(r)$ from which plasma parameters and the wave attenuation coefficient may be derived.

3. Calculation of the wave propagation characteristics

We assume that along the column, which is, in general, surrounded by coaxial layers of dielectric media, an azimuthally symmetric surface wave propagates. To calculate the wave propagation coefficient $\gamma=\alpha + j\beta$ ($j = \sqrt{-1}$) as a function of L, we consider a cylindrical column of homogeneous plasma characterised by the electric permittivity which is equal to the value averaged over the column cross-section of the radially variable permittivity calculated for given L. The cross-section average value of the complex relative permittivity is:

$$\varepsilon_p = \frac{1}{\pi a^2} \int_0^a 2\pi \varepsilon_p(r) r \,\mathrm{d}r \,. \tag{10}$$

For determination the local values of the plasma complex relative permittivity, $\varepsilon(r)$, the cold plasma linear dielectric approximation is used [25]:

$$\varepsilon_p(r) = 1 - \frac{\omega_p^2(r)}{\omega^2 + \nu^2(r)} - j \frac{\omega_p^2(r)}{\omega^2 + \nu^2(r)} \frac{\nu(r)}{\omega} \,, \tag{11}$$

where ω is the angular frequency of the wave, $\omega_p = ne^2/(\varepsilon_0 m_e)$ is the plasma frequency, e is the elementary charge, m_e – electron mass, ε_0 being the permittivity of vacuum.

To derive the dispersion equation, from which the propagation coefficient γ may be calculated, the wave equation is for the axial component of the electric field in the plasma column and each dielectric layer surrounding it:

$$\frac{1}{r}\frac{\partial}{\partial r}\left(r\frac{\partial E_z}{\partial r}\right)+\frac{1}{r^2}\frac{\partial^2 E_z}{\partial \varphi^2}+\frac{\partial^2 E_z}{\partial z^2}+\beta_0^2\varepsilon E_z=0 \tag{12}$$

where β_0 is the free-space phase coefficient of the wave. Solving these equations and imposing the usual boundary conditions on media interfaces one obtains a set of six homogeneous equations which has a single non-zero solution provided that its determinant is equal to zero. This condition yields the dispersion equation which, solved for consecutive values of L, provides the functional dependence $\alpha(L)$.

The next step is to substitute $\alpha(L)$ into equation (1) and solve it for the axial distribution $L(z)$ of the power loss per unit length. Finally, complete spatial distributions of plasma parameters are determined by merging $L(z)$ with the radial distributions calculated for given L. Further, we define (after [26]) the plasma column end as a place where $\alpha=\beta$. Therefore, the plasma column length ℓ can be calculated for any given value P_0.

4. Results of numerical calculations

The above described method has been applied to determination of the plasma parameters and the plasma column length in a SWD sustained at a frequency f=2.45 GHz in argon at atmospheric pressure. The fused silica discharge tube with the inner diameter $2a$=1 mm and the outer diameter $2b$=5 mm was used. The temperature at the outer wall of the tube was set to T=350 K. The calculations were performed for two cases: discharge tube is surrounded by air or it is surrounded by cooling coat of diameter 12 mm and shielding grid of diameter 46 mm. The presence of cooling coat and shielding grid does not affect the discharge processes but it changes the conditions of wave propagation. Cross sectionals view of the considered structure is depicted in Fig. 1.

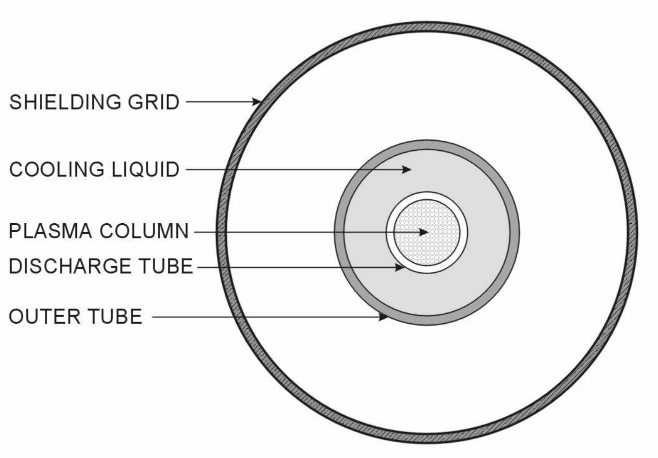

Fig. 1. Cross-section of the discharge setup.

Fig. 2 shows the calculated dependence of α on L in log-log coordinates. It can be seen that curves have similar shape and that, for values L lower than 1000 W/m, they can be approximated by linear function. The presence of additional dielectric layer (the cooling coat) increases the value of α for given value of L. In general, the attenuation increases when the electric permittivity and/or the thickness of the dielectric layer increases.

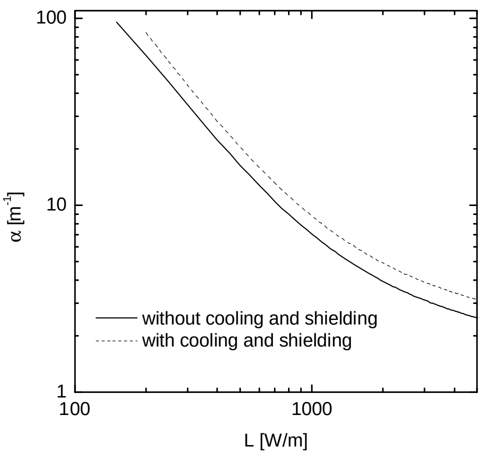

Fig. 2. Dependence of attenuation coefficient α on *L* for two cases: discharge tube is surrounded by cooling liquid and shielding grid – dotted line; discharge tube is surrounded by air – solid line.

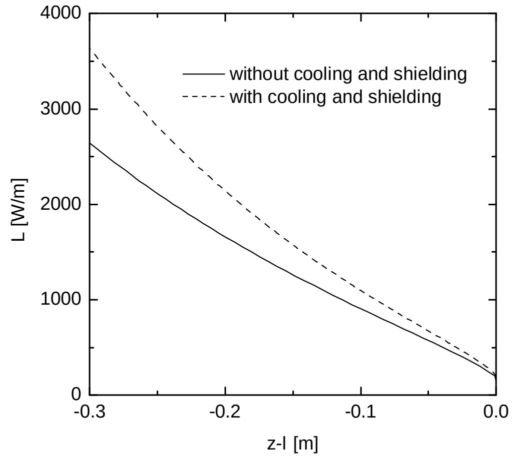

Fig. 3. Axial distribution of *L* for two cases: discharge tube is surrounded by cooling liquid and shielding grid – dotted line; discharge tube is surrounded by air – solid line.

In Fig. 3, the axial distributions of *L*, the power delivered from wave field to plasma per unit length, are presented. Both curves are almost linear but that with cooling and shielding is much steeper than the other one.

Fig. 4 shows the dependence of plasma column length on wave power. It could be seen that the column length rises with increasing power *P*. The existence of additional dielectric layer shortens the plasma column.

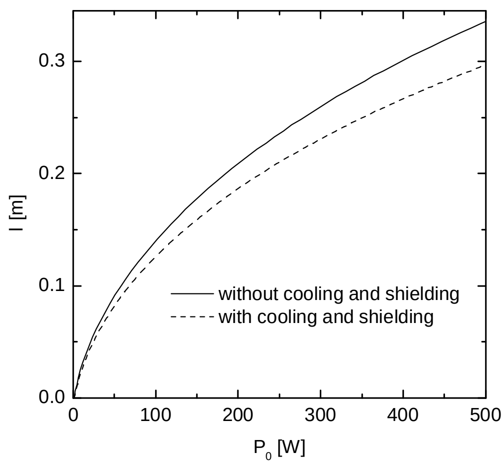

Fig. 4. Dependence of plasma column length on wave power for two cases: discharge tube is surrounded by cooling liquid and shielding grid – dotted line; discharge tube is surrounded by air – solid line.

5. Anatomy of a surface wave sustained discharge

Surface wave sustained discharges can be generated by using various kinds of high frequency applicators [4]. In a general case such a discharge has the structure as shown in Fig. 5. The microwave power is transferred from the electromagnetic field to the plasma in a wave launching region of axial dimension *d*. On both sides of that region extend plasma columns sustained by waves of SW nature while within it that nature has not been established yet. The model presented in the previous section can be applied separately to each of the columns but not to the wave launching region. In Fig. 5, $P_{01,2}$ and $l_{1,2}$ denote the microwave power at the beginning of the column and lengths of the columns, respectively, and indices 1, 2 refer to the column number. The total power absorbed in the discharge P_A is the sum of the power P_D, dissipated within launching region and the power necessary to sustain the plasma columns, $P_A = P_D + P_{01} + P_{02}$. In general case the lengths l_1 and l_2, differ depending on the wave launcher topology, gas flow, etc. In the case considered furtherdown in this paper, the only reason for the observed discharge axial asymmetry is the gas flow. Thus, we shall pay a particular attention to this aspect.

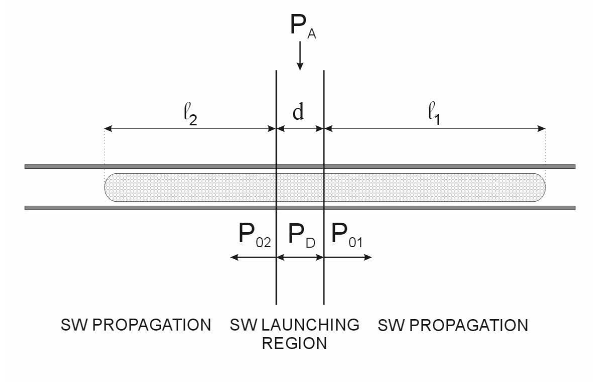

Fig. 5. Axial structure of a SWD.

6. Relation of the experimental result to the outcome of the modelling

Experiments yield only the total value of the power absorbed within the discharge, P_A, and values of $l_1+d/2$ and $l_2+d/2$. The extent of the launching region is not known. On the other hand, the model provides the dependence $l(P_0)$ of the single column length on the wave power at the column threshold. To perform an experimental verification of the model, one needs to determine the values of P_0 and l from available results of measurements. Let us concentrate on the question how it could be done.

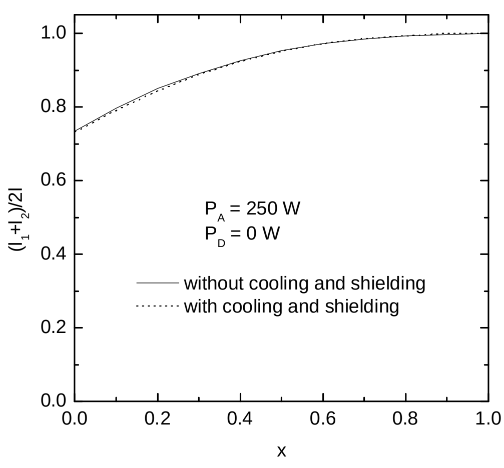

Fig. 6. Dependence of sum of plasma column lengths on $x = l_2/l_1$, for two cases: discharge tube is surrounded or not by cooling liquid and shielding grid.

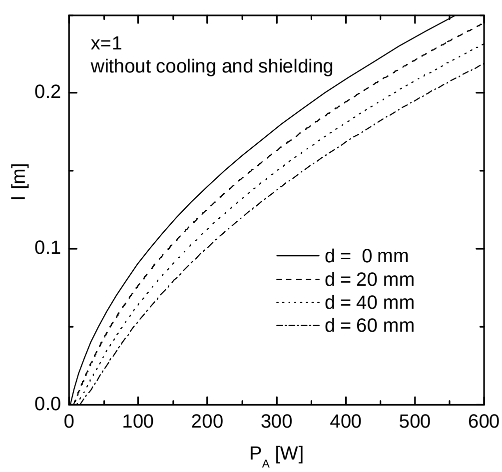

Fig. 7. Dependence of a single plasma column length on P_A, for different values of d.

In a particular case when the length d of the launching region can be assumed negligible with respect to l_1 and l_2, the experiment gives approximate values of l_1 and l_2 with $l_1>l$ and $l_2<l$, where l is the length of the single column of the symmetric discharge (no gas flow) at the same P_A.

The sum of the lengths l_1+l_2 depends not only on the absorbed power but also on the ratio $x= l_2/l_1$ of column lengths. This follows from the fact that the dependence $l(P_0)$ is not linear (Fig. 4). Fig. 6 shows how the value of l_1+l_2 changes with x for constant value of P_A. It is seen that for symmetric structure (x=1) the value of l_1+l_2 is maximal and the greater the deviation from the symmetry, the smaller is l_1+l_2. The smallest l_1+l_2 is when only single plasma column is generated (x=0). For x>0.5 the measured average column length $(l_1+l_2)/2$ is close to the column length of a symmetric discharge.

We approximate the power dissipated within the launching region as $P_D = L_D d$, i.e. as the product of dimension of the region (d), and average linear density of the power (L_D) which depends on P_A. In case of an axially symmetric discharge (no flow), $l_1=l_2=l$. Then the influence of the length d of the launching region on the length of a single column can be readily derived from our model. An example, corresponding to the conditions assumed in Section 4 is shown in Fig. 7.

7. Comparison between experimental results and calculations

The experiment was carried out at 2.45 GHz in a setup as that described in [27]. The discharge was sustained in argon flowing through a fused silica discharge tube of inner radius a=0.5 mm and outer radius b=2.6 mm and leaving it at p=1 bar directly to the ambient. This tube can be surrounded by a cooling coat of radius 6 mm and shielding metal grid of inner radius 23 mm. In such a structure two plasma columns are created by two SWs propagating in the opposite directions from the launching region. The length of the columns rises with increasing the power P. The axial symmetry of the discharge is disturbed by the flow of gas causing that the column sustained by the wave propagating in the direction of the flow is longer than the other one. Ratio of the column lengths depends on the intensity of the flow Q and varies from x=0.3 for Q=6 l/min to x=0.85 for Q=0.25 l/min.

The influence of the flow intensity on both columns length is shown in figure 8 for some values of absorbed power. It can be seen that in flow range from 0 to 4 l/mm the length of the longer column rises almost linearly with the flow, while length of the shorter column falls almost linearly with the flow. That means that from such data it is possible to estimate the asymptotic length of column of the limit when Q = 0 l/m, which as shown before is approximately equal to the average value of both plasma column lengths.

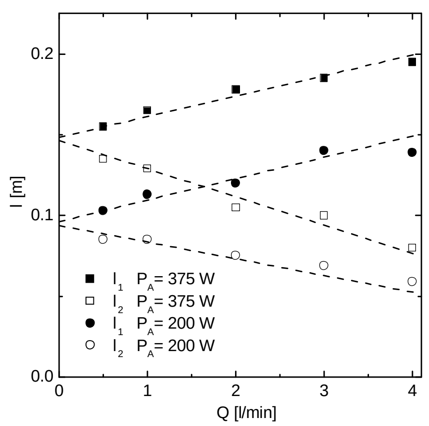

Fig. 8. Experimental values of column length vs intensity of gas flow for two values of absorbed power.

Figs. 9 and 10 show the dependence of the asymptotic value of the column lengths on the microwave power absorbed in the system for two cases: when the tube is surrounded by the cooling coat and shielding grid and when it is not. Calculated absorbed power is the sum of the wave power sustaining the plasma columns and the power absorbed in the launching region. We have estimated that for our applicator d=47 mm. The predicted values agree quite well with the experimental ones for small flows and differ for large flows. That is obvious because our model does not account for the flow.

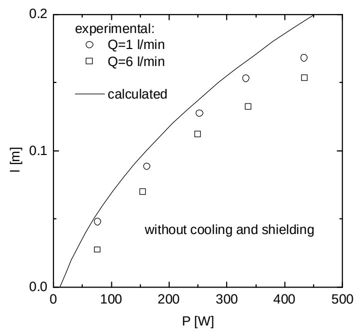

Fig. 9. The plasma column length vs absorbed power for case without cooling and shielding.

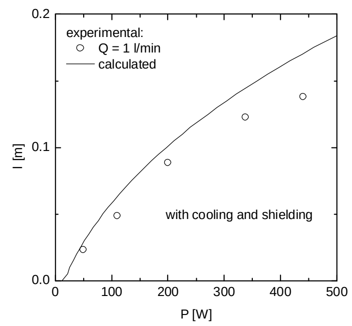

Fig. 10. The plasma column length vs absorbed power for case with cooling and shielding.

8. Conclusion

The dependence of l on P predicted by the model is in accordance with the experimental results for small flows and not for large flows, as our model does not account the flow. Also, as expected, the existence of cooling layer reduces the column length.

Acknowledgement

This work was supported by the State Committee for Scientific Research (KBN) under programme PB1124/T09/2003/24 and by the Polish Academy of Sciences under programme IMP O3/Z1/T1.

References

[1] C. M. Ferreira, J. Phys. D: Appl. Phys. **22**, 705 (1989).
[2] Z. Zakrzewski, M. Moisan, J. Phys. D: Appl. Phys. **24**, 1025 (1991).
[3] Z. Rakem, P. Leprince, J. Marec, J. Phys. D: Appl. Phys. **25**, 953 (1992).
[4] Z. Zakrzewski, M. Moisan, Plasma Sources Sci. Technol. **4**, 379 (1995).
[5] I. Zhelyazkov, V. Atanassov, Phys. Reports **225**, 81 (1995).
[6] E. Tatarova, F. M. Dias, C. M. Ferreira, A. Ricard, J. App. Physics, **85**, 49 (1999).
[7] V. Guerra, J. Loureiro, Plasma Sources Sci. and Technol. **8**, 110 (1999).
[8] Yu. M. Aliev, I. Ghanashev, H. Schlüter, A. Shivarova, M. Zethoff, Plasma Sources Sci. Technol. **3**, 216 (1994).
[9] V. Guerra, E. Tatarova, F. M. Dias, C. M. Ferreira, J. App. Phys. **91**, 2648 (2002).
[10] H. Nowakowska, Z. Zakrzewski, M. Moisan, J. Phys. D: Appl. Phys. **22**, 789 (1990).
[11] H. Nowakowska, Z. Zakrzewski, M. Moisan, M. Lubanski, J. Phys. D: Appl. Phys. **31**, 1422 (1998).
[12] V. M. Lelevkin, I. R. Rafatov, Vth International Workshop on Microwave Discharges; Fundamentals and Applications, Greifswald, July 8-12 (2003).
[13] I. R. Rafatov, V. M. Lelevkin, J. Phys. D: Appl. Phys. **37**, 2876 (2004).
[14] M. S. Benilov, G. V. Naidis, IEEE Trans. on Plasma Science **31**, 488 (2003).
[15] M. S. Benilov, G. V. Naidis, J. Phys. D: Appl. Phys. **36**, 1834 (2003).
[16] H. Nowakowska, Z. Zakrzewski, M. Moisan, J. Phys. D: Appl. Phys. **34**, 1474 (2001).
[17] G. V. Naidis, J. Phys. D: Appl. Phys. **34**, L103 (2002).
[18] Y. Kabouzi, M. D. Calzada, M. Moisan, K. C. Tran, C. Trassy, J. Appl. Phys. **91**, 1008 (2002).
[19] E. Castaños Martinez, Y. Kabouzi, K. Makasheva, M. Moisan, Phys. Rev. E **70**, 066405 (2004).
[20] V. M. Lelevkin, D. K. Otorbaev, D. C. Schram, Physics of non-equilibrium plasmas, North-Holland, Amsterdam (1992).
[21] G. M. Janssen, J. van Dijk, D. A. Benoy, M. A. Tas, K. T. A. L. Burm, W. J. Goedheer, J. A. M. van der Mullen, D.C. Schram, Plasma Sources Sci. Technol. **8**, 1 (1999).
[22] R. S. Devoto, Phys. Fluids **16**, 616 (1973).
[23] M. I. Bolous, P. Fauchais, E. Pfender, Thermal Plasmas Fundamentals and Applications, New York Plenum (1994).
[24] D. A. Benoy, J. A. M. van der Mullen, D. C. Schram, J. Quant. Spectrosc. Radiat. Transfer **46**, 195 (1991).
[25] V. L. Ginzburg, A. V. Gurevich, Usp. Fiz. Nauk **50**, 201 (1960) (in Russian).
[26] C. Boisse-Laporte, in: Microwave Discharges: Fundamentals and Applications, edited by C. M. Ferreira and M. Moisan (New York and London: Plenum Press) 25 (1993).
[27] M. Moisan, Z. Zakrzewski, R. Etemadi, J. C. Rostaing, J. Appl. Phys. **83**, 5691 (1998).